

Rod-Coating: Towards Large-Area Fabrication of Uniform Reduced Graphene Oxide Films for Flexible Touch Screens

Jie Wang, Minghui Liang, Yan Fang, Tengfei Qiu, Jin Zhang,* and Linjie Zhi*

Flexible transparent conductors (FTCs) are essential for a wide range of applications, including flexible touch screens and displays, printable electronics, flexible transistors, and thin-film photovoltaics.^[1–4] The dominant FTC used today is indium-doped tin oxide (ITO) coated on flexible substrates; however, besides the high cost and the scarcity of indium supply, ITO suffers from its ceramic nature as well,^[5] which limits its mechanical flexibility. Therefore, various materials, including metal grids or nanowires,^[6–8] conductive polymers,^[9] carbon nanotubes,^[2] and graphene,^[1] have been emerging as alternatives to ITO for FTCs. Among them, graphene has attracted great attention due to its 2D nature, high transparency, excellent electron-transfer behavior, chemical and thermal stability, low cost, and, more interestingly, its ultrahigh flexibility.^[10–12] Two important approaches have been developed to prepare graphene-based FTCs. One is a high-temperature method, using chemical vapor deposition to produce graphene on a hard substrate, followed by a transfer procedure to fabricate a graphene film on a flexible substrate;^[13–15] another approach is solution processing of dispersed graphene/graphene oxide directly on a flexible substrate.^[16–18]

The solution-processing approach is particularly interesting since it may fit into the roll-to-roll technique for continuous large-scale production of FTCs. Many methods have been developed to fabricate graphene-based films from solution, such as dip coating,^[3] vacuum filtration,^[19] spin-coating,^[20] spray-coating,^[21,22] Langmuir–Blodgett assembly,^[23] and self-assembly.^[24] However, continuous large-scale preparation of uniform graphene-based FTCs with high quality is still a big challenge. The critical issues are: a) the homogeneous dispersion of high-quality graphene in a solvent; b) the efficient chemical reduction of the graphene oxide film in the solid state; and c) a reproducible technique for continuous large-scale fabrication of graphene-based films. A combination of either (a) and (c) or (b) and (c) will result in a highly attractive strategy for roll-to-roll production of graphene-based FTCs. The development of a fast and reproducible method for solution processing of a graphene/graphene oxide dispersion

towards large-scale, uniform, and controllable graphene-based FTCs is therefore one of the critical issues for practical applications.

Herein, based on a highly efficient method developed in our group for the room-temperature reduction of solid-state graphene oxide (GO) films,^[25] we report a novel strategy to produce uniform reduced graphene oxide (RGO) films on a large scale directly on poly(ethylene terephthalate) (PET) substrates by using a rod-coating (Meyer rod) technique. Meyer rod-coating is a well-known coating technique that is widely used in the coating industry for making liquid thin films in a continuous and controlled manner.^[26] A Meyer rod is a metal bar with a wire wrapped around the outside that is used to draw a solution over a substrate surface. The diameter of the wire wrapped around the bar determines the thickness of the wet coating film. This technique can be used to coat directly onto PET, glass, and other substrates at room temperature and in a scalable way for roll-to-roll production in industry. Actually, rod-coating has been used successfully to fabricate silver nanowire films and even carbon nanotube films on a large scale.^[27,28] In this work, we report for the first time the combination of rod-coating and room-temperature reduction of graphene oxide films to produce scalably transparent and conductive RGO films directly on flexible substrates.

A typical wire-wound-rod setup for the lab-scale coating of GO films is shown in **Figure 1a**. A homogeneous GO solution passes through the groove between the wires when the rod moves over the substrate. The initial shape of the coating is a series of stripes, spaced apart from each other according to the spacing of the wire windings. Almost immediately, the normal surface tension pulls these stripes together, forming a flat, uniform film, ready for drying in air or under heat. In this work, GO was prepared according to the Hummers method.^[29] To obtain a suitable coating solution, the GO was dispersed in ethanol and ultrasonically (150 W, 40 kHz) treated for an hour before coating. The concentration of the GO dispersion used was 0.05–2.5 mg mL⁻¹. In the rod-coating, the rod moving speed was not a critical factor and could be adjusted in a small range.^[26] In our case, the coating speed was usually 150 mm s⁻¹, which enabled large and uniform GO films to be produced in a short time. **Figure 1b** shows a typical GO film (20 cm × 47 cm), deposited directly on a PET substrate by this method.

Using the rod-coating method, the thickness of GO films can be precisely controlled from a single layer to tens of layers by adjusting the concentration of the GO solution or the diameter of the rod wire. Atomic-force-microscopy (AFM) analysis was employed to characterize the thickness of the GO films deposited on Si substrates. In order to investigate the relationship between the thickness of the GO film and the concentration of the GO solution, a rod with a wire diameter of 0.2

J. Wang, M. Liang, Y. Fang, T. Qiu, Prof. L. Zhi
National Center for Nanoscience and Technology
Beiyitiao No. 11, Zhongguancun, Beijing, 100190, China
E-mail: zhilj@nanoctr.cn

J. Wang, Prof. J. Zhang
College of Chemistry and Molecular Engineering
Peking University
Beijing 100871, China
E-mail: jinzhang@pku.edu.cn



DOI: 10.1002/adma.201200055

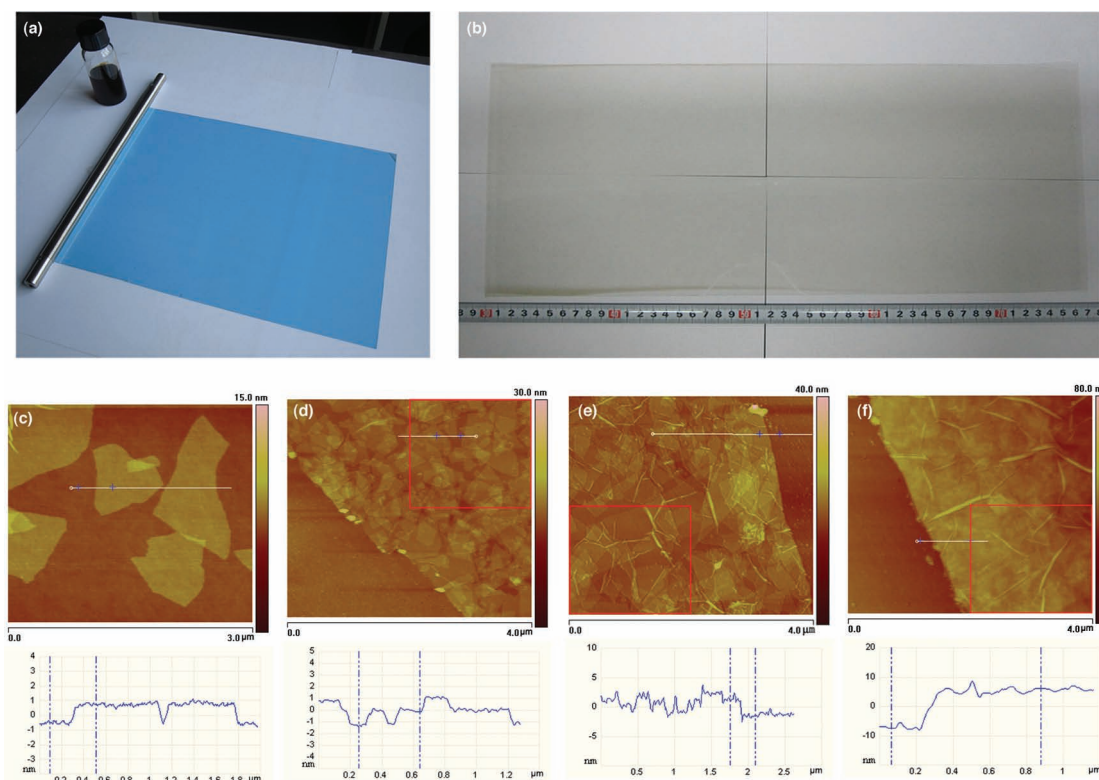


Figure 1. Fabrication of GO film by Meyer rod coating. a) Rod-coating setup. b) Photograph of a large-scale GO film deposited by rod-coating on PET (the background is four pieces of A4 paper). c–f) AFM images and height profiles of the GO films fabricated by rod-coating with different concentrations of GO dispersions: 0.05 mg mL⁻¹ (c); 0.1 mg mL⁻¹ (d); 0.2 mg mL⁻¹ (e); 1 mg mL⁻¹ (f). The diameter of the selected rod wire was 0.2 mm. The squares in Figure 1d–f demonstrate the area where the root-mean-square roughness of the film was obtained.

mm was selected. Figure 1c–f shows the AFM images and the height profiles of GO films prepared with GO concentrations of 0.05 mg mL⁻¹, 0.1 mg mL⁻¹, 0.2 mg mL⁻¹, and 1 mg mL⁻¹, respectively. For the GO film from the 0.05 mg mL⁻¹ solution, a very thin layer composed of isolated GO sheets was observed (Figure 1c), and the heights of the GO sheets were found to be 0.9–1.21 nm, corresponding to a single layer of GO. When the concentration of the GO solution was higher than 0.1 mg mL⁻¹, continuous and uniform GO films were obtained. The thicknesses of the prepared GO films from GO concentrations of 0.1 mg mL⁻¹, 0.2 mg mL⁻¹, and 1 mg mL⁻¹ were 1–2.4 nm, 2.0–3.6 nm, and 11.4–12.6 nm (Figure 1d–f), respectively, corresponding to 1–2 layers, 2–3 layers, and over 4 layers of GO film. These results are consistent with a previous report^[30] in which the thickness of one layer of GO film was 1.25 ± 0.8 nm, the thickness of two layers was 2.23 ± 0.11 nm, the thickness of three layers was 3.21 ± 0.21 nm, and the thickness of four layers was 4.26 ± 0.25 nm. The surface root-mean-square roughness (R_q) of the GO films was measured over selected areas of 4 μm², as shown in Figure 1d–f. The R_q values of the 3 films were 0.84 nm, 1.3 nm, and 2.13 nm, respectively, which were comparable to or even better than those of GO films prepared by other methods (Table S1, Supporting Information). As shown in Figure 2a (black squares), the thickness of the GO films, measured by AFM, had a linear relationship with the concentration of the GO dispersion in the range from 0.05 to 2.5 mg mL⁻¹. In

general, the final thickness of the GO film in our experiments could be approximated by the following equation:

$$h_{\text{GO}} = \frac{h_{\text{wet}} C}{\rho} \quad (1)$$

In Equation 1, h_{GO} is the final thickness of the GO film, h_{wet} is the thickness of the wet film (10% of the wire diameter used in our rod setup), C (mg mL⁻¹) is the concentration of the GO dispersion, and ρ is the density of the GO film (evaluated as 1.8 g cm⁻³).^[32] By using this method, the final thickness of the GO film can be tuned precisely and continuously from a single layer up to tens of layers.

To reduce a GO film into a conductive RGO film, we have developed an efficient method to reduce solid-state GO at room temperature by using hydrogen with the assistance of a small amount of a palladium (Pd) catalyst.^[25] A certain amount of palladium chloride (PdCl₂) was added into the GO solution (weight ratio of Pd to GO was 0.1) to form a stable dispersion that was then cast onto a PET film by rod-coating. After drying with flowing air, the GO film was reduced at room temperature in a pressured hydrogen system for 6 h. The sheet resistance and transmittance of the prepared RGO films on PET are shown in Figure 2b. Along with the increase of the GO concentration from 0.5 to 2.5 mg mL⁻¹, the transmittance of the RGO films decreased from 92.6% to 64.6% and the sheet

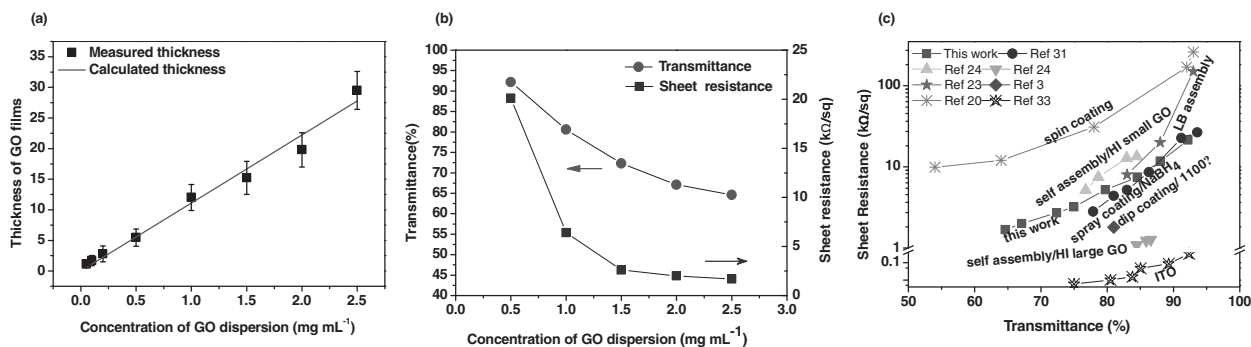


Figure 2. a) The thickness of the GO films (measured by AFM (black squares) and calculated using Equation 1 (the line) as a function of the concentration of the GO dispersion; the diameter of the selected rod wire was 0.2 mm. b) Optical and electrical properties of the RGO films formed by rod coating: sheet resistance and transmittance at 550 nm as a function of the concentration of the GO dispersion. c) The sheet resistance versus transmittance at 550 nm for various RGO films prepared by different methods and with ITO.^[31]

resistances dropped from 20.1 to 1.68 kΩ sq⁻¹. Compared with RGO films prepared by other coating methods,^[3,20,23,24,33] these films displayed competitive properties with regard to transparency and conductivity, as shown in Figure 2c. Generally speaking, the optical and electrical properties of RGO films depend strongly on the reduction method and the size of the GO precursors. Compared with our results, most of the RGO films prepared by other methods showed inferior or comparable properties, except for two examples that displayed slightly better properties. One was an RGO film prepared by dip-coating of GO and subsequent high-temperature treatment at 1100 °C, which showed a sheet resistance of 1.8 kΩ sq⁻¹

and a transmittance of 81%;^[3] another was an RGO film obtained through the hydroiodic acid (HI) reduction of large GO sheets (7000 μm²), which displayed a sheet resistance of 840 Ω sq⁻¹ and a transmittance of 78%.^[24] The average diameter of the as-prepared GO sheets used in our experiment was 40 μm (see Supporting Information Figure S2), and the reduction was conducted at room temperature directly on a flexible substrate. These results suggest that the rod-coating method combined with the catalytically induced hydrogen reduction of GO results in a simple and efficient approach to the production of flexible RGO films with good transparency and conductivity.

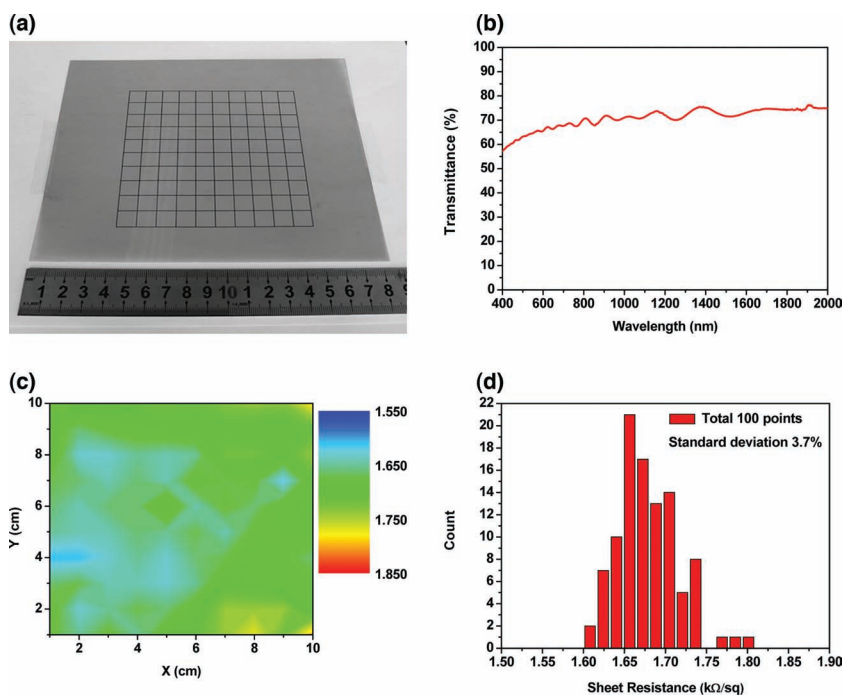


Figure 3. The uniformity of RGO/PET film prepared by rod coating. a) Photograph of the RGO film. b) Optical transmittance of the of the RGO film in the visible range. c) The spatial distribution of the sheet resistance on a 10 cm × 10 cm RGO/PET film. d) Distribution of the sheet resistances tested at 100 points.

The uniformity is another critical parameter for large-scale, flexible RGO films, particularly from the point of view of practical applications. For instance, in a four-wire resistive touch screen, the transparent electrode is required to have a uniform resistance, which is crucial for the fabrication of devices with good functionality, as it impacts on the linearity of the touch response.^[34] To evaluate the uniformity of the obtained RGO film on the PET substrate, 100 points over a 10 cm × 10 cm film were selected (in a 2D array with a 1 cm × 1 cm lattice) (Figure 3a) and were measured using the four-probe method (the spacing of the probes was 1 ± 0.01 mm). The selected RGO/PET film (deposited using 2.5 mg mL⁻¹ GO and a rod diameter of 0.2 mm) displayed a transmittance of 64.6% at 550 nm (Figure 3b). The spatial distribution of the sheet resistance of the film ranged from 1.55 kΩ sq⁻¹ (marked as blue) to 1.85 kΩ sq⁻¹ (marked as red) as shown in Figure 3c. Surprisingly, in most of the surface area, the green color was uniformly distributed, suggesting the sheet resistance in this area was mostly located between 1.65 and 1.75 kΩ sq⁻¹. The blue color corresponding to a sheet resistance of approximately 1.6 kΩ sq⁻¹ appeared in certain regions, and a

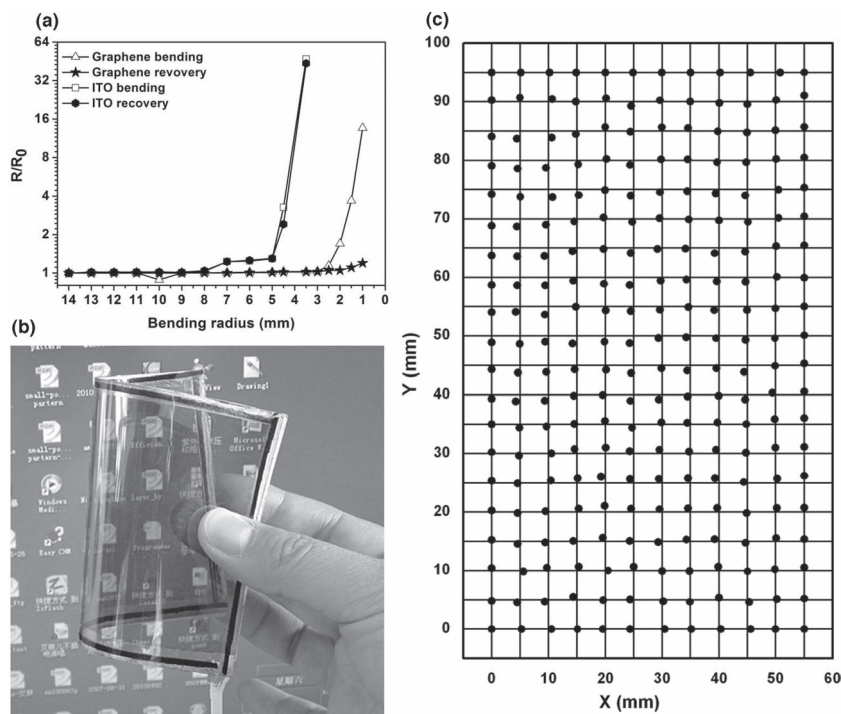


Figure 4. The mechanical properties of RGO film for flexible devices. a) The resistance change with tensile strain applied to RGO and ITO films on PET substrates under bending and unbending conditions. b) A flexible four-wire resistance touch screen fabricated using RGO/PET as electrodes. c) Linearity test of NC-FTS-1. The intersections of the lines indicate the practical touch points, and the black dots indicate the detected points.

small amount of yellow color was located at the edge area of the film. The standard deviation of the 100-point sheet resistance was 3.7% as shown in Figure 3d, well within the 10% specification required by the touch-panel industry.^[33] The uniformity of a typical thinner RGO film on PET (deposited using 1.4 mg mL⁻¹ GO and a rod diameter of 0.2 mm) with a transmittance of 75.4% (see Supporting Information Figure S3) was also tested, and the standard deviation was 9.8% over a 10 cm × 10 cm area, still within the range desired by the touch-screen manufacturers (generally <10%).^[33] It should be noted that the RGO films were prepared by hand-controlled rod-coating in our laboratory. We believe better results will be obtained on automated coating equipment, as would be standard in the coating industry.

The mechanical properties, particularly the foldability, of FTC films are another critical factor for flexible device applications.^[35] The foldability of the as-prepared RGO/PET film was examined by measuring its resistance change due to the decrease of the bending radius ranging from 14 to 1 mm (see Supporting Information Figure S5). For comparison, a commercialized ITO film on PET (0.188 μm, 400 Ω sq⁻¹) was examined in the same manner. **Figure 4a** shows the changes in the resistance of the RGO film and the ITO film at each of the bending radii. The resistance of the RGO/PET film remained virtually unperturbed by the bending (**Figure 4a**) up to a radius of 2.5 mm, and was perfectly recovered after unbending. Although the sheet resistance increased to a value 14 times higher than the original one at a bending radius of 1 mm, it recovered to a value 1.2 times the original one after unbending. In contrast,

Figure 4a shows the typical behavior of the ITO/PET film under bending conditions. For bending radii from 14 to 8 mm, the resistance of the ITO kept constant, and then a steady increase of the resistance (by a factor of 3) was observed with the decrease of the bending radius to 4.5 mm. More importantly, a dramatic increase of the resistance (by a factor of 47) of the ITO/PET film occurred immediately, at a bending radius of 3.5 mm. The recovery of the film resistance was almost impossible after unbending, with a value still 43 times higher than the original one. These results demonstrate the excellent flexibility of RGO/PET films. These facts can be associated with the pristine structures of ITO and RGO films. For the brittle ITO films, cracks occurred under bending to disconnect the films, while the RGO film was composed of overlapping 2D RGO sheets, which introduced little resistance increase when bending.

Based on its excellent flexibility and good transparency and conductivity, the as-prepared RGO/PET films were used successfully as electrodes for the fabrication of flexible four-wire resistance touch screens. Since these screens were first-generation screens based on RGO electrodes in our lab, they were named NC-FTS-1. The structure of the NC-FTS-1 is shown in **Figure S6** (Supporting Information). This flexible touch screen (FTS)

performed the functions of touch screens, while also exhibiting mechanical flexibility, as shown in **Figure 4b**. Even after high-angle bending, the NC-FTS-1 still worked very well and no function decay was observed (for a video of the bending and the function of NC-FTS-1, see the Supporting Information).

For practical applications, accurate positioning is a basic requirement towards high-performance touch screens, which is commonly determined by linearity testing. The linearity of our NC-FTS-1 was tested by measuring the voltage gradient of the touch position at intervals of 5 mm in the *x* and *y* directions, respectively, according to Jiang's method^[36] (see the Supporting Information). For the NC-FTS-1, the linearity was 1.4% on the *x* axis and 1.2% on the *y* axis, which is comparable to that of mechanical ITO touch screens. For conventional ITO-based touch screens, the linearity should be less than 1.5%.^[37] **Figure 4c** shows the detected points (the crossing points of the lines) and the touch points (the black dots). It can be seen clearly that every detected point sits near the same site as its corresponding touch point. The good linearity of NC-FTS-1 further proves the uniformity and stability of the as-prepared RGO films. Based on these results, it is expected that the Meyer rod-coating technique is highly promising for large-scale production of RGO-based FTC films for flexible touch-screen applications on an industrial-production level.

In summary, the rod-coating technique has been successfully demonstrated to fabricate a large-scale GO film in a controllable manner on both PET and Si substrates. By combining this technique with a newly developed room-temperature reduction

method, highly flexible RGO films with a low resistance and good transparency have been prepared directly on PET substrates. The uniformity of the sheet resistance of the prepared RGO films was compatible with industry expectations, exhibiting a standard deviation of 3.7–9.8% over 100 cm². A fully functional 4.5 inch four-wire resistance touch screen was successfully fabricated using the as-prepared RGO/PET film as the electrodes. It showed not only a linearity comparable to ITO-based touch screens, but also a high mechanical flexibility exceeding that of ITO-based touch screens. Thus, this work demonstrates an approach potentially suitable for the roll-to-roll production of usable RGO films for various flexible electronic devices.

Experimental Section

Preparation of Graphene Oxide Suspensions: All of the reagents used were of analytical-reagent degree. Graphene oxide (GO) was prepared from natural flake graphite using a modified Hummers method. Typically, graphite (2 g), sodium nitrate (2 g), and potassium permanganate (6.0 g) were mixed in 98% sulfuric acid (96 mL) by vigorous agitation in a round-bottom flask at 0 °C for 24 h. Then, the water bath was heated and kept at 35 °C for 1 h. After that, distilled water (500 mL) was slowly added into the suspension and stirred for 20 min before hydrogen peroxide (5 mL, 30%) was added. The as-prepared solution was washed thoroughly with deionized water using low-speed centrifugation (3000 rpm) to remove the visible particles. The supernatant was then centrifuged at high-speed (8000 rpm, 30 min) until its pH was ≈7. The obtained precipitates were redispersed in deionized water to obtain a GO dispersion (10 mg mL⁻¹) for further use.

Preparation of Reduced Graphene Oxide Films: There were three steps used to prepare the reduced graphene oxide (RGO) film. 1) Preparation of GO and palladium chloride suspension: in a typical experiment, 1 mL of a GO dispersion (10 mg mL⁻¹) and 0.2 mL of palladium chloride aqueous solution (Pd content: 5 mg mL⁻¹) were dispersed in 8.8 mL of ethanol to obtain a homogeneous GO/Pd solution (GO/Pd mass ratio = 9:1). 2) Deposition of GO/Pd film by rod-coating: 1 mL of the GO/Pd solution was dropped on the edge area of a PET substrate, and a Meyer rod (0.2 mm, Pushen) was pulled over the solution at a speed of 150 mm s⁻¹, leaving a uniform wet film that was then dried with flowing air (0.5 m s⁻¹). 3) Reduction of the GO/Pd film by hydrogen: the reduction of the film was executed in an autoclave pressurized with hydrogen at room temperature for 6 h. The palladium was removed by immersing the film in a HCl/H₂O₂ solution for 10 min, and the film was then dried at 80 °C for further use.

Supporting Information

Supporting Information is available from the Wiley Online Library or from the author.

Acknowledgements

Financial support from the National Natural Science Foundation of China (Grant No. 20973044, 21173057), the Ministry of Science and Technology of China (No. 2009AA03Z328, No. 2009DPA41220 and No. 2012CB933403), the Chinese Academy of Sciences (No. KJCX2-YW-H21), and the Guangdong-CAS Strategic Co-operation Program (2009B091300007) is acknowledged.

Received: January 5, 2012

Revised: February 28, 2012

Published online: April 27, 2012

- [1] S. Bae, H. Kim, Y. Lee, X. Xu, J. S. Park, Y. Zheng, J. Balakrishnan, T. Lei, R. H. Kim, Y. I. Song, Y. J. Kim, K. S. Kim, B. Ozyilmaz, J. Ahn, B. H. Hong, S. Iijima, *Nat. Nanotechnol.* **2010**, *5*, 574.
- [2] E. Artukovic, M. Kaempgen, D. S. Hecht, S. Roth, G. Gruner, *Nano Lett.* **2005**, *5*, 757.
- [3] X. Wang, L. J. Zhi, K. Mullen, *Nano Lett.* **2008**, *8*, 323.
- [4] D. S. Hecht, L. Hu, G. Irvin, *Adv. Mater.* **2011**, *23*, 1482.
- [5] Z. N. Yu, Y. Q. Li, F. Xia, W. Xue, *Surf. Coat. Technol.* **2009**, *204*, 131.
- [6] M. G. Kang, M. S. Kim, J. S. Kim, L. J. Guo, *Adv. Mater.* **2008**, *20*, 4624.
- [7] J. Y. Lee, S. T. Connor, Y. Cui, P. Peumans, *Nano Lett.* **2008**, *8*, 689.
- [8] H. Wu, L. Hu, M. W. Rowell, D. Kong, J. J. Cha, J. R. McDonough, J. Zhu, Y. Yang, M. D. McGehee, Y. Cui, *Nano Lett.* **2010**, *10*, 4242.
- [9] S. I. Na, S. S. Kim, J. Jo, D. Y. Kim, *Adv. Mater.* **2008**, *20*, 4061.
- [10] K. S. Novoselov, A. K. Geim, S. V. Morozov, D. Jiang, Y. Zhang, S. V. Dubonos, I. V. Grigorieva, A. A. Firsov, *Science* **2004**, *306*, 666.
- [11] K. I. Bolotin, K. J. Sikes, Z. Jiang, M. Klima, G. Fudenberg, J. Hone, P. Kim, H. L. Stormer, *Solid State Commun.* **2008**, *146*, 351.
- [12] C. Lee, X. D. Wei, J. W. Kysar, J. Hone, *Science* **2008**, *321*, 385.
- [13] X. S. Li, W. W. Cai, J. H. An, S. Kim, J. Nah, D. X. Yang, R. Piner, A. Velamakanni, I. Jung, E. Tutuc, S. K. Banerjee, L. Colombo, R. S. Ruoff, *Science* **2009**, *324*, 1312.
- [14] A. Reina, X. T. Jia, J. Ho, D. Nezich, H. B. Son, V. Bulovic, M. S. Dresselhaus, J. Kong, *Nano Lett.* **2009**, *9*, 30.
- [15] Z. Z. Sun, Z. Yan, J. Yao, E. Beitler, Y. Zhu, J. M. Tour, *Nature* **2010**, *468*, 549.
- [16] S. Stankovich, D. A. Dikin, R. D. Piner, K. A. Kohlhaas, A. Kleinhammes, Y. Jia, Y. Wu, S. T. Nguyen, R. S. Ruoff, *Carbon* **2007**, *45*, 1558.
- [17] I. K. Moon, J. Lee, R. S. Ruoff, H. Lee, *Nat. Commun.* **2010**, *1*, 73.
- [18] N. Behabtu, J. R. Lomed, M. J. Green, A. L. Higginbotham, A. Sinitskii, D. V. Kosynkin, D. Tsentralovich, A. N. G. Parra-Vasquez, J. Schmidt, E. Kesselman, Y. Cohen, Y. Talmon, J. M. Tour, M. Pasquali, *Nat. Nanotechnol.* **2010**, *5*, 406.
- [19] G. Eda, G. Fanchini, M. Chhowalla, *Nat. Nanotechnol.* **2008**, *3*, 270.
- [20] H. A. Becerril, J. Mao, Z. Liu, R. M. Stoltenberg, Z. Bao, Y. Chen, *ACS Nano* **2008**, *2*, 463.
- [21] S. Gilje, S. Han, M. Wang, K. L. Wang, R. B. Kaner, *Nano Lett.* **2007**, *7*, 3394.
- [22] V. H. Pham, T. V. Cuong, S. H. Hur, E. W. Shin, J. S. Kim, J. S. Chung, E. J. Kim, *Carbon* **2010**, *48*, 1945.
- [23] X. L. Li, G. Y. Zhang, X. D. Bai, X. M. Sun, X. R. Wang, E. Wang, H. J. Dai, *Nat. Nanotechnol.* **2008**, *3*, 538.
- [24] J. Zhao, S. Pei, W. Ren, L. Gao, H. M. Cheng, *ACS Nano* **2010**, *4*, 5245.
- [25] M. Liang, J. Wang, B. Luo, T. Qiu, L. Zhi, *Small* **2012**, *8*, 1180.
- [26] D. M. Macleod, in *Coatings Technology: Fundamentals, Testing, and Processing Techniques*, (Ed: A. A. Tracton), CRC Press, Boca Raton, FL **2007**, Ch. 19.
- [27] B. Dan, G. C. Irvin, M. Pasquali, *ACS Nano* **2009**, *3*, 835.
- [28] L. Hu, H. S. Kim, J. Y. Lee, P. Peumans, Y. Cui, *ACS Nano* **2010**, *4*, 2955.
- [29] W. S. Hummers, R. E. Offeman, *J. Am. Chem. Soc.* **1958**, *80*, 1339.
- [30] I. Jung, M. Pelton, R. Piner, D. A. Dikin, S. Stankovich, S. Watcharotone, M. Hausner, R. S. Ruoff, *Nano Lett.* **2007**, *7*, 3569.
- [31] J. Y. Lee, S. T. Connor, Y. Cui, P. Peumans, *Nano Lett.* **2008**, *8*, 689.
- [32] D. A. Dikin, S. Stankovich, E. J. Zimney, R. D. Piner, G. H. B. Dommett, G. Evmenenko, S. T. Nguyen, R. S. Ruoff, *Nature* **2007**, *448*, 457.
- [33] H. J. Shin, K. K. Kim, A. Benayad, S. M. Yoon, H. K. Park, I. S. Jung, M. H. Jin, H. K. Jeong, J. M. Kim, J. Y. Choi, Y. H. Lee, *Adv. Funct. Mater.* **2009**, *19*, 1987.
- [34] D. S. Hecht, D. Thomas, L. Hu, C. Ladous, T. Lam, Y. Park, G. Irvin, P. Drzaic, *J. Soc. Inf. Display* **2009**, *17*, 941.
- [35] J. Lewis, *Mater. Today* **2006**, *9*, 38.
- [36] C. Feng, K. Liu, J. S. Wu, L. Liu, J. S. Cheng, Y. Y. Zhang, Y. H. Sun, Q. Q. Li, S. S. Fan, K. L. Jiang, *Adv. Funct. Mater.* **2010**, *20*, 885.
- [37] Y. Iwabuchi, M. Nishida, Y. Kusano, (Bridgestone Corporation, JP), US 6787253 **2004**.